VIP Reaction Mechanisms

DOI: 10.1002/anie.201104623

The Molecular Mechanism of Enzymatic Glycosyl Transfer with Retention of Configuration: Evidence for a Short-Lived Oxocarbenium-Like Species**

*Albert Ardèvol and Carme Rovira**

The catalytic mechanism of nucleotide-sugar-dependent glycosyltransferases (GTs), especially those that act with retention of anomeric configuration, remains one of the most intriguing unanswered questions in the field of glycobiology. In contrast to the well-characterized mechanistic strategies used by glycoside hydrolases (GHs) to catalyze the cleavage of glycosidic bonds,[1] the mechanisms of retaining GTs remain unclear. GTs catalyze glycosyl group transfer with either inversion or retention of the anomeric stereochemistry with respect to the donor sugar.[2] The mechanism of inverting GTs is clearly established: an S_N2 reaction in a single displacement step with a general base catalyst that increases the nucleophility of the attacking group,[2] analogous to that of inverting GHs. In contrast, the mechanism of retaining GTs remains controversial. Double-displacement mechanisms have been proposed by analogy to retaining GHs.[3] Indeed, evidence of the formation of covalent glycosyl–enzyme adducts (Scheme 1, top) has been reported for some fold-type A GTs (family 6 mammalian α-3-galactosyltransferase, α3GalT and blood group GTs) by means of chemical rescue,[4] mass spectrometry,[5] and theoretical calculations.[6] Another scenario is that of GTs for which a putative nucleophile protein residue has not been proposed, such as glycogen phosphorylase, a retaining GT that does not use nucleotide-sugars,[7] lipopolysaccharyl α-galactosyltransferase (LgtC), and trehalose-6-phosphate synthase (OtsA). This prompted some authors to suggest an unusual mechanism (Scheme 1, bottom),[8] in which the reaction proceeds by a front-side single displacement, similar to the solvolysis reaction of glycosyl fluoride[9] that was regarded early on as a type of S_Ni or "internal return" mechanism. In this mechanism, the nucleophilic hydroxy group of the acceptor attacks the anomeric carbon atom from the same side from which the leaving group departs, thus explaining the retention of stereochemistry. Early theoretical analyses on simplified gas-phase models of the active site of LgtC showed that this is a possible mechanism and that it takes place in one step.[10] Other authors have further elaborated on this idea,[2,11] thereby alluding to a mechanism in which a short-lived oxocarbenium-like species is formed, thus avoiding the high steric strain expected for a S_Ni mechanism. In this respect, the reaction could also be regarded as a type of S_N1 reaction in which the outgoing leaving group enhances the basicity of the acceptor nucleophile.

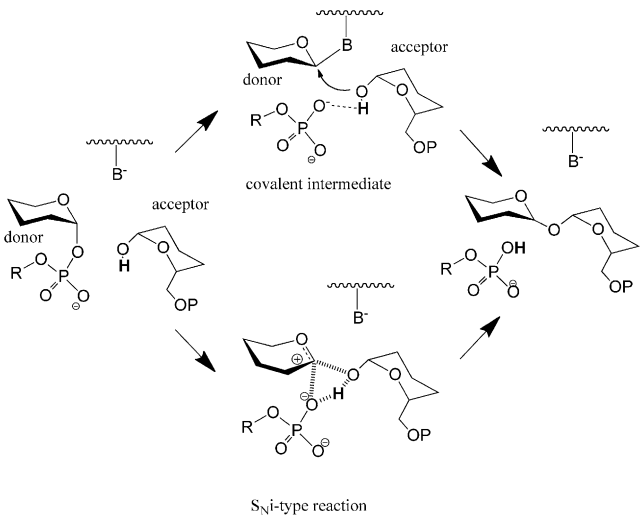

Scheme 1. Possible reaction mechanisms for enzymatic glycosyl transfer with retention of configuration proposed in the literature. The donor and acceptor molecules are those of OtsA. Bonds partially formed/cleaved are indicated by a hashed line. Hydroxymethyl and hydroxy substituents of Glc are omitted for clarity.

OtsA is a classical glycosyltransferase of the GT-B fold that catalyzes the formation of the α,α-1,1 linkage between uridyldiphosphate glucose (UDP-Glc) and glucose-6-phosphate (Glc-6P), thus leading to trehalose-6-phosphate. A recent structural study of OtsA inhibitor complexes[12] shows that there is a hydrogen bond between the amine of the inhibitor (to be replaced by the O1' for the natural substrate) and the UDP, thereby suggesting that the phosphate group acts as a Brønsted base in the glycosyl-transfer reaction. This gives support to a S_Ni-type mechanism (Scheme 1, bottom), without excluding the presence of a metastable (i.e. short

[*] A. Ardèvol, Prof. C. Rovira
Computer Simulation and Modeling Laboratory (CoSMoLAB),
Parc Científic de Barcelona
Baldiri Reixac 10–12, 08028 Barcelona (Spain)
E-mail: crovira@pcb.ub.es
Prof. C. Rovira
Institució Catalana de Recerca i Estudis Avançats (ICREA)
Passeig Lluís Companys 23, 08020 Barcelona (Spain)

[**] We thank Prof. A. Planas, Prof. B. G. Davis, and Dr. S. S. Lee for enlightening discussions on the mechanisms of GTs. This work was funded by the MICINN (FIS2008-03845) and GENCAT (2009SGR-1309). A.A. thanks MEC for a FPU studentship. We acknowledge the computer support, technical expertise, and assistance provided by the Barcelona Supercomputing Center-Centro Nacional de Supercomputación (BSC-CNS).

Supporting information for this article is available on the WWW under http://dx.doi.org/10.1002/anie.201104623.

lived) oxocarbenium-like intermediate (using the IUPAC recommended nomenclature, the latter is defined as $D_N{*}A_{Nss}$ mechanism).[2] A recent kinetic isotope labeling and linear free-energy relationship investigation[13] gives further support for this type of mechanism. However, a current lack of mechanistic insight does not allow conclusions regarding the molecular details of the mechanism.

Here we use quantum mechanics/molecular mechanics (QM/MM)[14] metadynamics simulations (see Experimental Section) to decipher the reaction mechanism of trehalose-6-phosphate synthase (OtsA). Metadynamics[15] is a powerful technique for enhancing the sampling in molecular dynamics simulations and reconstructing the free-energy surface (FES) as a function of a few selected degrees of freedom (collective variables, CVs). It has been previously applied with success to decipher enzyme reaction mechanisms,[16] including the hydrolysis of glycosidic bonds by GHs.[17]

A major barrier to the model study of OtsA (and GTs in general) is the limited structural data for the ternary complex between the enzyme, the donor, and the acceptor residues (UDP-Glc and Glc-6P in OtsA). Among the complexes that were recently reported by Errey et al.,[12] there is one [OtsA complex with UDP and validoxylamine-6-phosphate (VA6P)] that structurally resembles one of the reaction products (trehalose-6-phosphate). Therefore, we took this ternary OtsA complex with VA6P and UDP (PDB 2WTX) to construct the natural products of the reaction (trehalose-6-phosphate and UDP) and the Michaelis complex (see Experimental Section).

The metadynamics simulation of the glycosyl-transfer reaction was initiated from the modeled Michaelis complex (Figure 1). Functions of the C1···O_P-UDP, the C1···O1′ acceptor, and the O-H···O_P-UDP distances were considered as collective variables (see Scheme 2 and page 4 of the Supporting Information). The first collective variable (CV_1) is the difference in coordination number (CN) between the anomeric carbon atom of the donor with the phosphate oxygen atom (O_P) minus the O1′ ($CV_1 = CN_{C1,O_P} - CN_{C1,O'}$). The second collective variable (CV_2) involves the O1′, H, and O_P atoms in a similar way ($CV_2 = CN_{O1',H} - CN_{O_P,H}$). Therefore, CV_1 describes the cleavage of the glucose–UDP covalent bond and the formation of the glycosidic bond, while CV_2 describes the proton transfer from the acceptor molecule to the phosphate group.

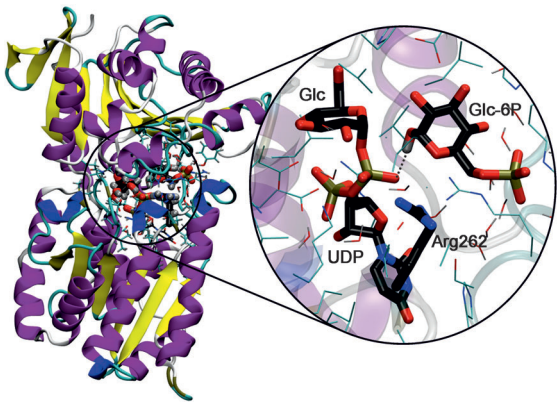

Figure 1. Ternary complex of OtsA·with UDP·and Glc-6P complex obtained from the calculations. The atoms of the QM region are shown in licorice representation (H atoms have been omitted for clarity). Picture generated with VMD.[18]

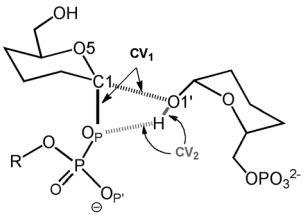

Scheme 2. Collective variables used in the QM/MM metadynamics simulations.

The free-energy surface reconstructed from the metadynamics simulation is shown in Figure 2. The two most stable minima are the reactants (in the upper left corner) and the products (in the lower right corner). The reactants well is 23 kcal mol^{-1} below the maximum point along the minimum energy reaction pathway, which is in reasonable agreement with the values obtained from experimental measurements of the reaction rate constants for retaining GTs (17–20 kcal mol^{-1}).[4,5,13,19] The energy barrier is also similar to the ones reported for glycosyl hydrolases investigated with a similar computational methodology.[17]

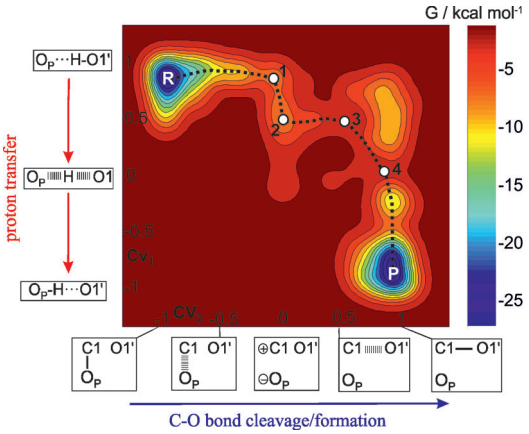

Figure 2. Computed free-energy landscape with respect to the two collective variables described in the text. Each contour line corresponds to 2 kcal mol^{-1}.

A detailed description of the reaction can be obtained by following the minimum free-energy pathway.[20] Figure 3 shows representative snapshots of relevant configurations along this pathway. At the reactants state (**R**), which corresponds to the Michaelis complex, there is a hydrogen bond between the O1′ acceptor atom and one of the nonbridging UDP oxygen atoms ($O_{P'}$). Consequently, the distance between the H atom and the leaving phosphate oxygen atom (O_P) is rather long (O_P···H > 2.5 Å, Figure 4 and Table S1 in the Supporting Information). The reaction starts with the elongation of the C–O bond between the UDP and the glucose molecule of the donor (e.g., the C1–O_P increases

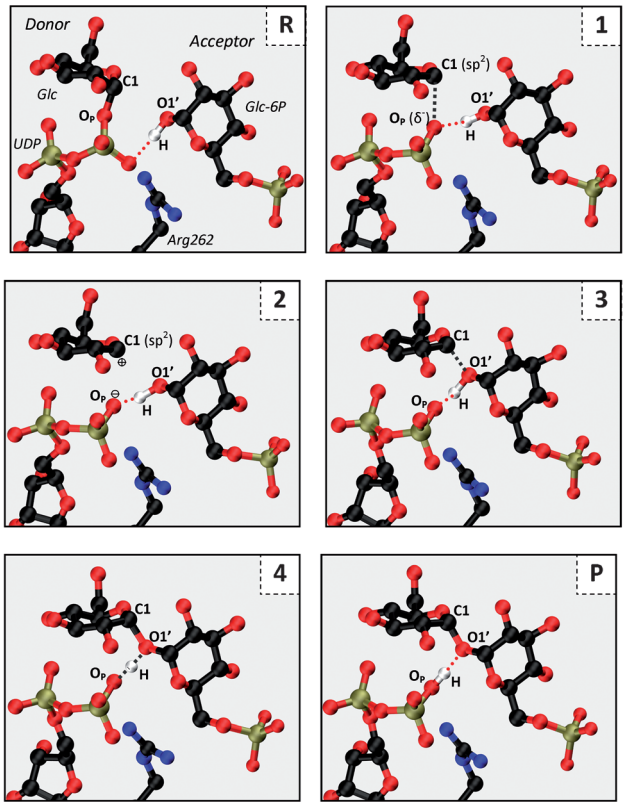

Figure 3. Atomic rearrangement along the reaction pathway. Hydrogen atoms have been omitted for clarity, except the one being transferred from the sugar acceptor to the UDP phosphate group. Bonds being broken/formed are represented by a dotted black line (configurations **1**, **3**, and **4**), whereas the crucial donor···acceptor hydrogen bond is represented by a dotted red line.

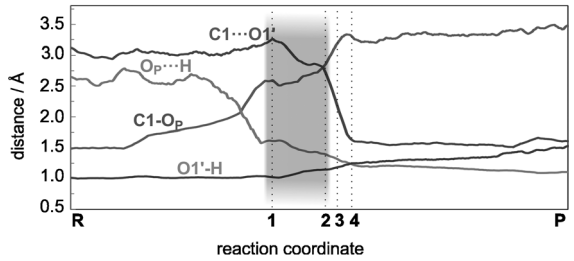

Figure 4. Evolution of the most relevant distances involving the donor and acceptor (see atom labeling in Scheme 2) along the reaction coordinate of Figure 3. Each distance is an average from all configurations falling into a small region around the corresponding point of the FES. The separation among the labeled points (**R**, **1**, **2**, **3**, **4**, and **P**) depends on the number of structures sampled in the metadynamics simulation and thus is not proportional to the distance among these points in the FES.

more than 1 Å when going from **R** to **1**). Simultaneously, the O1′–H bond changes its hydrogen-bond partner, from $O_{P'}$ to O_P (see for example, the dramatic decrease in the O_P···H distance from 2.5 Å to 1.6 Å, Figure 4 and Table S1 in the Supporting Information), thus placing the hydrogen atom at the proper position to assist the departure of the UDP leaving group. The O1′-H···O_P hydrogen bond not only stabilizes the negative charge being developed at the phosphate group, but it also places the acceptor molecule in a position that favors the forthcoming front side nucleophilic attack. Therefore, the first part of the reaction can be described as the cleavage of the C1–O_P bond together with the formation of a hydrogen bond between the acceptor and the phosphate oxygen atom of the bond being broken.

The C1–O_P bond becomes completely broken at **2** (C1-O_P = 2.84 Å; see Table S1 in the Supporting Information). Remarkably, the distance between the donor and the acceptor (C1-O1′) is still rather long (2.79 Å), thus indicating the presence of an oxocarbenium–phosphate ion pair. In fact, there is a portion of the reaction pathway (i.e., the shadowed region in Figure 4) in which both O_P and O1′ atoms are quite separated from the anomeric carbon atom (> 2.5 Å). All complexes in this region, which expands around **1** and **2**, approximately, can be taken as representatives of oxocarbenium-like species. Further evidence for the sp^3 to sp^2 change in the hybridization of the anomeric carbon atom is the conformational change of the glucose ring from the $^4C_1$ chair in the reactants to a $^4H_3$ half-chair conformation (the C2, C1, O5, and C5 atoms are almost coplanar) in **1, 2**, and **3**. This change is accompanied by a decrease of the intraring C1–O5 distance (from 1.39 to 1.28 Å; see Table S1 in the Supporting Information) and an increase of the charge of the anomeric center (by 0.45 e when going from from **R** to **2**; see Figure S6 in the Supporting Information). These structural changes are in remarkable agreement with recent kinetic isotope-labeling experiments, which indicate that a species with substantial oxocarbenium character and the pyranose ring flattened through C5-O5-C1-C2, forms.[13]

The decrease of CV_2 when going from **1** to **2** reflects the increasing contribution of the O1′-H···O_P hydrogen bond to the phosphate–oxocarbenium ion-pair stabilization. In fact, the H···O_P distance becomes quite short at **2** (1.38 Å). Afterward, a slight displacement of the glucose donor and acceptor molecules takes place (see Figure S4 in the Supporting Information), thus facilitating the interaction between the C1 and O1′ atoms in **3**. Concomitant with the formation of the C1–O1′ bond, the proton transfers to the phosphate group (**4**; the proton is shared between O1′ and O_P). The process **3**→**4**→**P** (**P** = products) is thus the formation of the donor–acceptor glycosidic bond in concert with the protonation of the UDP phosphate group.

Several conclusions can be drawn from the above mechanistic analysis. Firstly, the cleavage of the glucose–UDP bond (C1–O_P) and the formation of the donor–acceptor bond (C1–O1′) are highly asynchronous. The cleavage of the UDP–Glc bond precedes the formation of the Glc–Glc bond and thus an intimate ion-pair intermediate is formed. Secondly, there is a crucial participation of the acceptor hydrogen atom during the whole process. At the first stage of the reaction, the acceptor hydrogen atom interacts with the O_P atom, thus assisting the departure of the UDP leaving group. In the second stage, it transfers to the phosphate group, thereby enhancing the nucleophilicity of the acceptor sugar O1′ and thus facilitating the formation of the donor–acceptor glycosidic bond. In fact, an additional simulation not including the H···O_P interaction as part of the collective variables (see the Supporting Information) resulted in a much higher

free-energy barrier. We thus conclude that the critical stabilizing interaction of the acceptor hydrogen atom with the UDP leaving group acts as a driving force for the reaction.

The FES of Figure 2 could be interpreted, in principle, as a two-step mechanism (similar to that of a S_N1 reaction) in which an oxocarbenium ion-pair intermediate forms. However, the energy differences among configurations **1**–**4** are very small (± 2 kcal mol^{-1}). Notably, such a flat reaction free-energy profile was already hypothesized by Sinnott and Jencks for the solvolysis of D-glucosyl fluoride by mixtures of ethanol and trifluorethanol.[9] The oxocarbenium (**1**–**3**) corresponds to just a shallow minimum in the free energy profile (see also Figure S5 in the Supporting Information) and, therefore, it represents an extremely short-lived species. As a further characterization of this species, we extracted several snapshots of the metadynamics simulation that correspond to structures around **1** and **2** and performed geometry optimizations and subsequent room temperature ab initio molecular dynamics simulations. Although the ion-pair species turned out to be stable under optimization, in all cases the structure evolved either towards reactants or towards products within a few picoseconds of molecular dynamics. This again indicates that the ion-pair species is extremely short-lived and, as such, it should be very difficult to trap experimentally.

It is also important to point out that the identification of a unique transition-state structure for the enzymatic reaction is, in this case, not trivial. The highest point along the free-energy pathway corresponds to the formation of the Glc–Glc bond (**3**), but most of the activation energy is invested in breaking the UDP–Glc bond (**R**$\rightarrow$**1**). As mentioned above, there is a wide window along the reaction pathway (from **1** to **4**, approximately) in which the free energy does not change significantly. Any structure in this region can be taken as being representative of the transition state and therefore an experimental measurement aimed at characterizing the transition state would probably reflect a mixture of all configurations. The transition-state-like inhibitor of Errey et al., for instance, resembles configuration **4** from its donor–acceptor covalent bond distance. Our calculations suggest that molecules with a longer donor–acceptor bond, that is, moving towards configuration **3** (C1$-$O1′$\approx$2 Å) in the FES, such as those with a thioglycosidic bond, might also be good inhibitors.

In summary, our QM/MM metadynamics simulations support a single displacement but two-step type of mechanism with a very short lived ion-pair intermediate for the formation of trehalose-6-phosphate from UDP–Glc and Glc–6P catalyzed by OtsA. This process, which can be regarded as a type of S_Ni reaction or a S_N1 with an extremely short-lived intermediate, is in remarkable agreement with the proposals of recent kinetic and structural studies on OtsA.[12–13] Altogether, our results show that glycosyl transfer with retention of the anomeric configuration can take place in the absence of a protein nucleophile, provided that a hydrogen atom of the acceptor is properly oriented to assist the cleavage of the Glc–UDP bond. It would be extremely interesting to probe whether this mechanism is also possible for glycosyltransferases that, unlike OtsA, have a putative nucleophile residue near the anomeric carbon atom, such as α3GalT[4] and blood group GTs,[5] that is, whether the mechanism highlighted in this study can compete with the proposed S_N2 reaction for these GTs. These studies are underway in our laboratory.

Experimental Section

Methods: QM/MM calculations were performed using the method developed by Laio et al.,[21] which combines Car-Parrinello MD,[22] based on DFT, with force-field MD. The QM/MM interface was modeled by the use of a link-atom pseudopotential that saturates the QM region.[23] The electrostatic interactions between the QM and MM regions were handled by a fully Hamiltonian coupling scheme, where the short-range electrostatic interactions between the QM and the MM regions are explicitly taken into account for all atoms[14] (see Supporting Information for further details). The PBE functional[24] in the generalized gradient-corrected approximation of Density Functional Theory (DFT) was selected in view of its good performance in previous works on glycosidases.[17a,c,25]

The enzyme complex with thehalose-6-phosphate and UDP (i.e. the natural product) was used to generate the Michaelis complex of the reaction (i.e. the OtsA·UDP-Glc·Glc-6P ternary complex, for which there is no crystal structure available), using the following procedure. Starting with the product complex (i.e. the OtsA·UDP·-trehalose-6P), we performed 5 ns of classical molecular dynamics simulations at 300 K using the AMBER force-field (see the Supporting Information for full details), followed by 6.4 ps of QM/MM molecular dynamics simulation. The QM region included the trehalose-6-P, part of the UDP (the two phosphate groups), as well as the side chain of Arg262, which interacts with one of the phosphate UDP groups (72 QM atoms, 18319 MM atoms). The resulting computed structure of the OtsA·UDP·trehalose-6P complex turned out to be in very good agreement with the X-ray structure of the OtsA- VA6P complex (Figure S1 in the Supporting Information). Afterwards, the Michaelis complex was obtained by the cleavage of the glycosidic bond and the formation of the Glc–UDP bond in two steps, using the metadynamics algorithm (see details in the Supporting Information). The resulting structure (Figure 1) turned out to be in very good agreement with its most related experimental structure available (see Figure S3 in the Supporting Information), which is that of the binary complex of OtsA with a 2-fluoro-Glc-UDP inhibitor (PDB code 1UQT), thus proving the reliability of the model. Additional computational details are given in the Supporting Information.

Received: July 5, 2011
Published online: September 26, 2011

Keywords: computational chemistry · glycosides · reaction mechanisms · transferases · transition states

[1] D. J. Vocadlo, G. J. Davies, *Curr. Opin. Chem. Biol.* **2008**, *12*, 539–555.
[2] L. L. Lairson, B. Henrissat, G. J. Davies, S. G. Withers, *Annu. Rev. Biochem.* **2008**, *77*, 521–555.
[3] L. N. Gastinel, C. Bignon, A. K. Misra, O. Hindsgaul, J. H. Shaper, D. H. Joziasse, *EMBO J.* **2001**, *20*, 638–649.
[4] A. Monegal, A. Planas, *J. Am. Chem. Soc.* **2006**, *128*, 16030–16031.
[5] N. Soya, Y. Fang, M. M. Palcic, J. S. Klassen, *Glycobiology* **2011**, *21*, 547–552.
[6] I. Andre, I. Tvaroska, J. P. Carver, *Carbohydr. Res.* **2003**, *338*, 865–877.
[7] M. L. Sinnott, *Chem. Rev.* **1990**, *90*, 1171–1202.
[8] K. Persson, H. D. Ly, M. Dieckelmann, W. W. Wakarchuk, S. G. Withers, N. C. Strynadka, *Nat. Struct. Biol.* **2001**, *8*, 166–175.

[9] M. L. Sinnott, W. P. Jencks, *J. Am. Chem. Soc.* **1980**, *102*, 2026 – 2032.
[10] a) I. Tvaroška, *Carbohydr. Res.* **2004**, *339*, 1007 – 1014; b) I. Tvaroska in *Molecular modeling of retaining glycosyltransferases*, *Vol. 930* (Eds.: J. F. G. Vliegenthart, R. J. Woods), American Chemical Society, Washington, **2006**, pp. 285 – 301.
[11] C. Goedl and B. Nidetzky, *ChemBioChem* **2009**, *10*, 2333 – 2337.
[12] J. C. Errey, S. S. Lee, R. P. Gibson, C. Martinez Fleites, C. S. Barry, P. M. Jung, A. C. O'Sullivan, B. G. Davis, G. J. Davies, *Angew. Chem.* **2010**, *122*, 1256 – 1259; *Angew. Chem. Int. Ed.* **2010**, *49*, 1234 – 1237.
[13] S. S. Lee, S. Y. Hong, J. C. Errey, A. Izumi, G. J. Davies, B. G. Davis, *Nat. Chem. Biol.* **2011**, DOI: 10.1038/NChemBio.1628.
[14] A. Warshel, M. Levitt, *J. Mol. Biol.* **1976**, *103*, 227 – 249.
[15] A. Laio, M. Parrinello, *Proc. Natl. Acad. Sci. USA* **2002**, *99*, 12562 – 12566.
[16] a) M. Boero, T. Ikeda, E. Ito, K. Terakura, *J. Am. Chem. Soc.* **2006**, *128*, 16798 – 16807; b) V. Leone, F. Marinelli, P. Carloni, M. Parrinello, *Curr. Opin. Struct. Biol.* **2010**, *20*, 148 – 154.
[17] a) L. Petersen, A. Ardevol, C. Rovira, P. J. Reilly, *J. Phys. Chem. B* **2009**, *113*, 7331 – 7339; b) L. Petersen, A. Ardevol, C. Rovira, P. J. Reilly, *J. Am. Chem. Soc.* **2010**, *132*, 8291 – 8300; c) I. J. Barker, L. Petersen, P. J. Reilly, *J. Phys. Chem. B* **2010**, *114*, 15389 – 15393.
[18] W. Humphrey, A. Dalke, K. Schulten, *J. Mol. Graph.* **1996**, *14*, 33 – 38.
[19] H. S. Seo, Y. J. Koo, J. Y. Lim, J. T. Song, C. H. Kim, J. K. Kim, J. S. Lee, Y. D. Choi, *Appl. Environ. Microbiol.* **2000**, *66*, 2484 – 2490.
[20] K. Fukui, *Acc. Chem. Res.* **1981**, *14*, 363 – 368.
[21] A. Laio, J. VandeVondele, U. Rothlisberger, *J. Chem. Phys.* **2002**, *116*, 6941 – 6947.
[22] R. Car, M. Parrinello, *Phys. Rev. Lett.* **1985**, *55*, 2471 – 2474.
[23] Y. K. Zhang, T. S. Lee, W. T. Yang, *J. Chem. Phys.* **1999**, *110*, 46 – 54.
[24] J. P. Perdew, K. Burke, M. Ernzerhof, *Phys. Rev. Lett.* **1996**, *77*, 3865 – 3868.
[25] X. Biarnes, J. Nieto, A. Planas, C. Rovira, *J. Biol. Chem.* **2006**, *281*, 1432 – 1441.

